Postsynaptic GABABRs Inhibit L-Type Calcium Channels and Abolish Long-Term Potentiation in Hippocampal Somatostatin Interneurons

Report

Cell Reports

Postsynaptic $GABA_B$Rs Inhibit L-Type Calcium Channels and Abolish Long-Term Potentiation in Hippocampal Somatostatin Interneurons

Graphical Abstract

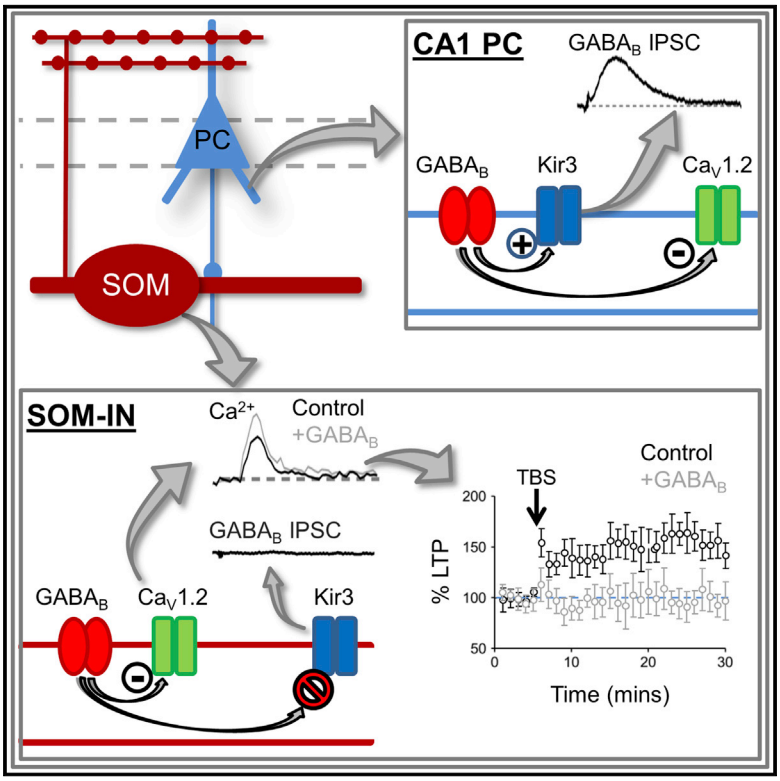

Authors

Sam A. Booker, Desiree Loreth, Annabelle L. Gee, ..., David J.A. Wyllie, Ákos Kulik, Imre Vida

Correspondence

akos.kulik@physiologie.uni-freiburg.de (Á.K.),
imre.vida@charite.de (I.V.)

In Brief

Booker et al. show that $GABA_B$ receptors are highly expressed on somatostatin interneuron dendrites. Rather than activating Kir3 channels, they preferentially co-cluster with, and negatively couple to, L-type calcium channels inhibiting long-term potentiation at excitatory inputs.

Highlights

- $GABA_B$ receptors do not activate Kir3-currents in CA1 somatostatin interneurons
- In somatostatin interneurons, $GABA_B$ receptors inhibit dendritic L-type Ca^{2+} channels
- $Ca_V1.2$ channels co-cluster with $GABA_{B1}$ on somatostatin interneuron dendrites
- $GABA_B$ activation abolishes long-term potentiation in somatostatin interneurons

Booker et al., 2018, Cell Reports *22*, 36–43
January 2, 2018
https://doi.org/10.1016/j.celrep.2017.12.021

CellPress

OPEN ACCESS
CellPress

Cell Reports
Report

Postsynaptic $GABA_BRs$ Inhibit L-Type Calcium Channels and Abolish Long-Term Potentiation in Hippocampal Somatostatin Interneurons

Sam A. Booker,[1,3,4,5,7] Desiree Loreth,[2] Annabelle L. Gee,[7] Masahiko Watanabe,[6] Peter C. Kind,[3,4,5] David J.A. Wyllie,[3,4,5] Ákos Kulik,[2,8,*] and Imre Vida[1,7,9,*]

[1]Institute for Integrative Neuroanatomy, NeuroCure Cluster of Excellence, Charité - Universitätmedizin Berlin, 10117 Berlin, Germany
[2]Institute of Physiology, Faculty of Medicine, University of Freiburg, Hermann-Herder-Str. 7, 79104 Freiburg, Germany
[3]Centre for Discovery Brain Sciences, University of Edinburgh, Edinburgh, UK
[4]Simons Initiative for the Developing Brain, University of Edinburgh, Edinburgh, UK
[5]Patrick Wild Centre for Autism Research, University of Edinburgh, Edinburgh, UK
[6]Department of Anatomy, Graduate School of Medicine, Hokkaido University, Sapporo 0608638, Japan
[7]Institute for Neuroscience, Glasgow University, Glasgow G12 8QQ, UK
[8]Centre for Biological Signalling Studies (BIOSS), University of Freiburg, Schänzle-Str. 18, 79104 Freiburg, Germany
[9]Lead Contact
*Correspondence: akos.kulik@physiologie.uni-freiburg.de (Á.K.), imre.vida@charite.de (I.V.)
https://doi.org/10.1016/j.celrep.2017.12.021

SUMMARY

Inhibition provided by local GABAergic interneurons (INs) activates ionotropic $GABA_A$ and metabotropic $GABA_B$ receptors ($GABA_BRs$). Despite $GABA_BRs$ representing a major source of inhibition, little is known of their function in distinct IN subtypes. Here, we show that, while the archetypal dendritic-inhibitory somatostatin-expressing INs (SOM-INs) possess high levels of $GABA_BR$ on their somato-dendritic surface, they fail to produce significant postsynaptic inhibitory currents. Instead, $GABA_BRs$ selectively inhibit dendritic $Ca_V1.2$ (L-type) Ca^{2+} channels on SOM-IN dendrites, leading to reduced calcium influx and loss of long-term potentiation at excitatory input synapses onto these INs. These data provide a mechanism by which $GABA_BRs$ can contribute to disinhibition and control the efficacy of extrinsic inputs to hippocampal networks.

INTRODUCTION

Maintained balance of excitation and inhibition controlled by feedforward and feedback interneurons (INs) is essential for appropriate function of cortical networks. Despite recruitment of local INs being critical to this balance, the contributing cellular mechanisms remain largely unexplored. Somatostatin (SOM) expressing INs constitute a dominant feedback inhibitory element in cortical circuits. In hippocampal CA1, SOM-INs are characterized by a somato-dendritic domain confined to *stratum* (*str.*) *oriens* and an axon providing inhibition to distal dendrites of pyramidal cells (PCs) in *str. lacunosum-moleculare*, as such they are referred to as O-LM cells (McBain et al., 1994; Katona et al., 1999; Müller and Remy, 2014). SOM-INs gate extrinsic cortical inputs into CA1 (Leão et al., 2012) and contribute to the generation of network oscillations at theta frequencies (Gloveli et al., 2005; Klausberger and Somogyi, 2008), with known roles in neuropathology (de Lanerolle et al., 1989; Dugladze et al., 2007; Wang et al., 2011). SOM-INs are recruited by recurrent input from CA1 PCs, involving ionotropic α-amino-3-hydroxy-5-methyl-4-isoxazolepropionic acid (AMPA) (Topolnik et al., 2005; Lamsa et al., 2007), N-methyl-D-aspartate (NMDA) (Standaert et al., 1996), and group 1 metabotropic glutamate receptors (mGluRs), particularly mGluR1α (Baude et al., 1993; McBain et al., 1994; Topolnik et al., 2006). Group I mGluRs on SOM-INs activate $Ca_V1.2$ (L-type) high voltage-gated Ca^{2+} channels (VGCCs), promoting synaptic plasticity at excitatory inputs (Topolnik et al., 2009; Nicholson and Kullmann, 2014).

While glutamatergic mechanisms have been well characterized, inhibitory control of SOM-INs is less well understood (Tyan et al., 2014). In particular, little is known regarding the effects of metabotropic $GABA_BRs$, despite $GABA_{B1}$ subunits being highly expressed at SOM-IN somata (Sloviter et al., 1999). In this study, we used whole-cell recording, 2-photon Ca^{2+}-imaging, and high-resolution quantitative SDS-digested freeze-fracture replica (SDS-FRL) immunoelectron microscopy to examine postsynaptic $GABA_BR$ function and localization in SOM-INs.

RESULTS

To determine whether SOM-INs possess functional $GABA_BRs$, we performed whole-cell recordings from rat acute hippocampal slices. CA1 SOM-INs were located in *str. oriens/alveus* with horizontal dendrites (Figure 1A) and responded with a large voltage "sag" to hyperpolarizing currents and minimally adapting action potential (AP) trains to depolarizing currents (Figure 1A, inset). All INs tested were immunoreactive for SOM (155 INs), of which 64 (41.3%) were identified as O-LM cells and 3 (1.9%) were bistratified INs. The remaining 88 (56.8%) were not morphologically identified due to the axon being cut, but were included in further

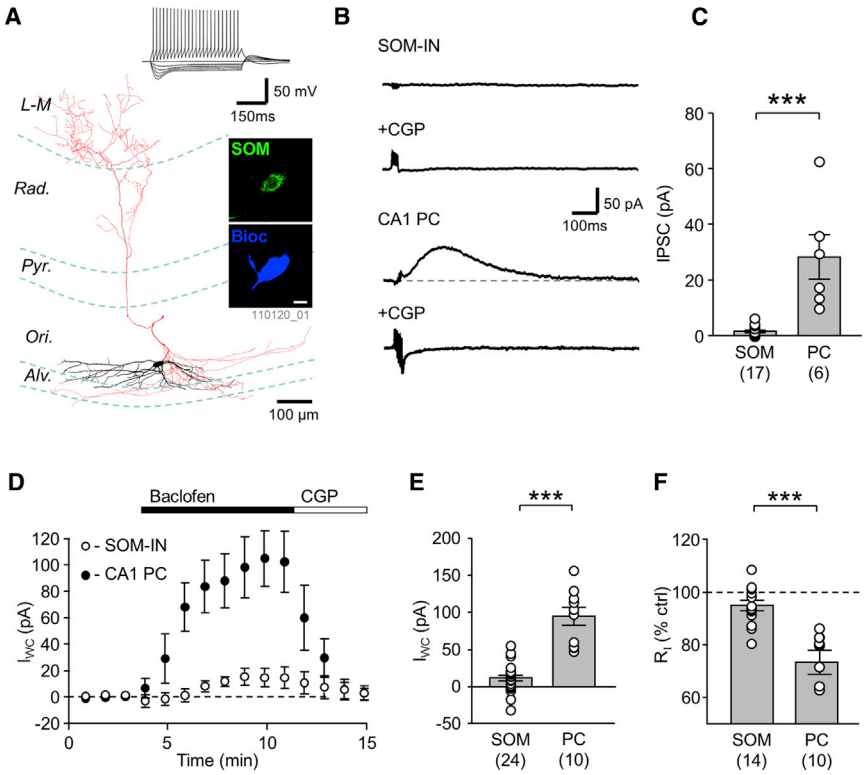

Figure 1. Postsynaptic $GABA_BR$-Mediated sIPSCs and Whole-Cell Currents Are Small in SOM-INs

(A) Reconstruction of a CA1 SOM-IN (black, dendrites; red, axon). Right inset: immunoreactivity for SOM (green) at the IN soma (blue; scale bar, 10 µm). Top inset: voltage response of the cell to hyper- to depolarizing current pulses (−500 to 500 pA, 500 ms).

(B) Pharmacologically isolated sIPSCs evoked by stimulation to *str. oriens* in a SOM-IN (top) and CA1 PC (bottom), blocked by CGP-55,845 (CGP; 5 µM, bottom traces).

(C) Bar chart of $GABA_BR$ sIPSC amplitudes in SOM-INs and CA1 PCs.

(D) Time course of I_{WC} following application of baclofen (10 µM) and CGP in SOM-INs (open circles) and CA1 PCs (filled circles).

(E and F) Summary charts of the changes in I_{WC} (E) and normalized input resistance (R_I) (F) during baclofen application in SOM-INs and CA1 PCs.

Bar charts show mean ± SEM. Open circles correspond to individual data; cell numbers are in parentheses. ***$p < 0.001$.

See also Figures S1 and S2.

analysis. CA1 PCs were recorded as controls, given their well described functional $GABA_BR$ expression (Lüscher et al., 1997).

$GABA_BR$-Mediated IPSCs Are Small in SOM-INs

Hippocampal neurons possess slow $GABA_BR$-mediated inhibitory postsynaptic currents (sIPSCs), elicited by extracellular stimulation (Degro et al., 2015). In SOM-INs, trains of stimuli (5 at 200 Hz) to *str. oriens* in the presence of $GABA_A$, NMDA, and AMPA receptor blockers produced very small or no sIPSC (Figures 1B, upper, and 1C). The mean sIPSC amplitude was 1.8 ± 0.5 pA (17 cells) and when present was blocked by the $GABA_BR$ antagonist CGP-55,845 (CGP, 10 cells). In CA1 PCs, sIPSCs were markedly larger with a mean amplitude of 28.3 ± 8.8 pA (6 cells, $U_{(17,6)} = 0$; $p < 0.0001$, Mann-Whitney test) (Figures 1B and 1C) and were also blocked by CGP (Figure 1B, bottom), excluding technical limitations affecting SOM-IN recordings. A subset of recordings were performed in adult rats (9 cells, P50–P60) that confirmed that $GABA_BRs$ minimally activate K^+ currents in SOM-INs (Figure S1).

Endogenous release of GABA activates only a proportion of the cells' $GABA_BR$ complement (Lüscher et al., 1997; Degro et al., 2015). Therefore, we next measured whole-cell currents (I_{WC}) produced by the $GABA_BR$ agonist baclofen. Bath-applied baclofen (10 µM) produced only a small outward I_{WC} in SOM-INs (12.1 ± 4.0 pA, 24 cells), which was fully reversed by subsequent CGP application (Figure 1D). The same activation in CA1 PCs produced a robust I_{WC} of 94.9 ± 12.7 pA (10 cells), ~8-fold larger than SOM-INs ($U_{(24,10)} = 3.0$; $p < 0.0001$, Mann-Whitney test) (Figures 1D and 1E). This I_{WC} was accompanied by a marked reduction in input resistance from 130 ± 13 MΩ to 95 ± 11 MΩ in CA1 PCs (10 cells) consistent with channel opening. In contrast, only a small change from 207 ± 14 MΩ to 195 ± 13 MΩ was observed in SOM-INs (14 cells; $U_{(14,10)} = 4.0$; $p < 0.0001$, Mann-Whitney test) (Figure 1F). These findings were further validated by briefly activating $GABA_BRs$ through uncaging of GABA over the dendrites of SOM-INs and CA1 PCs (Figure S2A), which resulted in currents of 6.4 ± 2.6 pA (5 cells) and 93.7 ± 23.4 pA (6 cells), respectively ($U_{(5,6)} = 0$; $p = 0.0043$, Mann-Whitney test) (Figures S2B and S2C). In summary, the $GABA_BR$-mediated inhibitory conductance in SOM-INs is an order of magnitude lower than CA1 PCs, indicating that $GABA_BR$/Kir3 signaling does not significantly contribute to SOM-IN inhibition.

$GABA_BRs$ Strongly Inhibit Dendritic L-Type VGCCs

The absence of $GABA_BR$-mediated currents in SOM-INs suggests that the receptors may signal through an alternative effector, such as high voltage-gated $Ca_V1.2$ (L-type) Ca^{2+} channels (Chalifoux and Carter, 2011) known to contribute to signaling and plasticity in SOM-INs (Topolnik et al., 2006). To determine whether $GABA_BRs$ inhibit $Ca_V1.2$ in SOM-INs, we performed 2-photon imaging of IN dendrites filled with a morphometric and a Ca^{2+}-indicator dye and evoked short trains of back-propagating APs (bAPs, 4× at 200 Hz) (Figure 2A). Imaging a primary dendrite with rapid line-scans, we observed large Ca^{2+}-transients in response to bAPs (Figures 2B and 2C), which had a ΔF/F of 31.5% ± 3.7% (17 cells). These transients were stable for the 20-min recording (4 cells) (Figure S3A) and blocked by $CdCl_2$ (5 mM, 3 cells) (Figure S3B) and did not differ during baseline for any test group ($R^2_{(5,4,6)} = 0.04$; $p = 0.78$, one-way ANOVA). Baclofen applied to SOM-INs

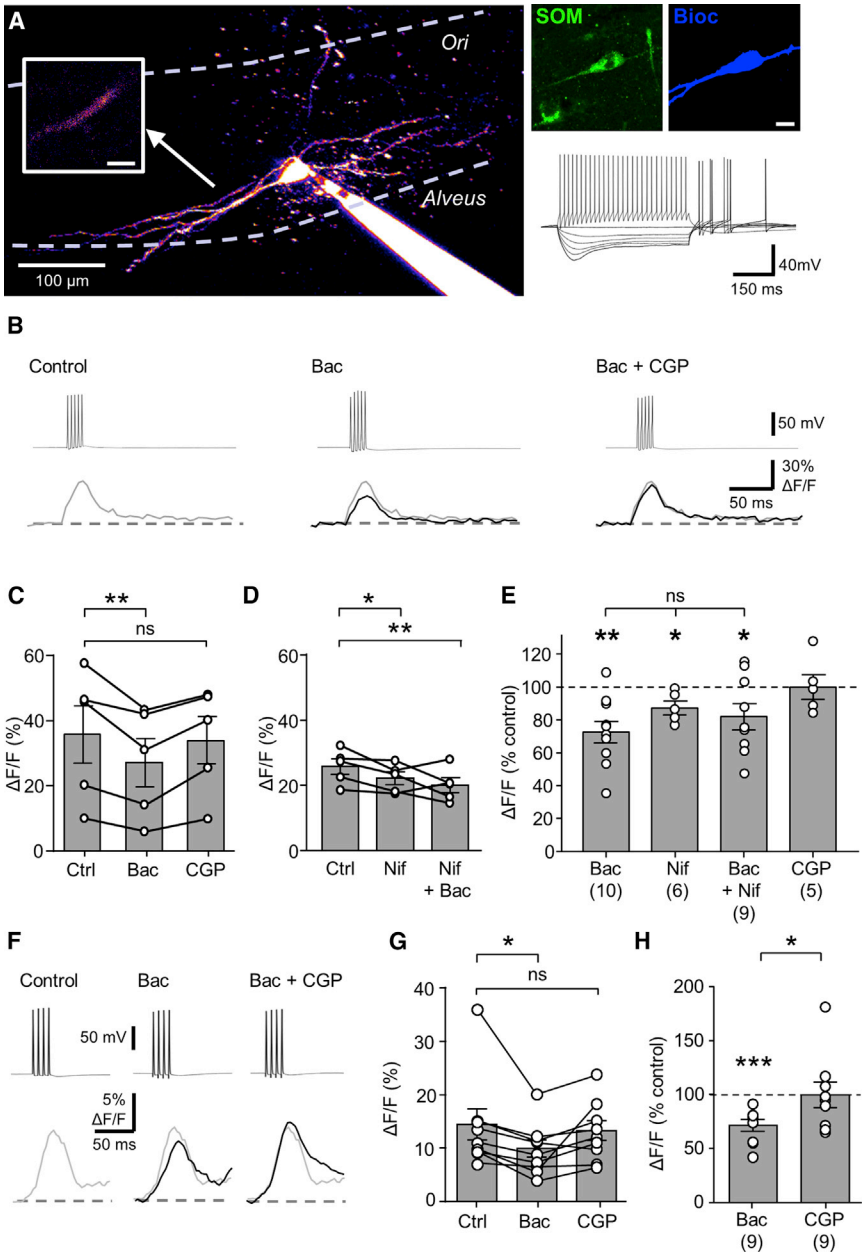

Figure 2. $GABA_BRs$ Inhibit L-Type VGCC-Mediated Ca^2-Transients in SOM-IN Dendrites

(A) A 2-photon image of a SOM-IN filled with Alexa Fluor 594 (morphometric dye) and BAPTA-OGB1 (100 µM for Ca^{2+}-imaging) and the imaged proximal dendritic segment (inset). Top right: confocal images confirm immunolabeling for SOM (green, left) at the soma (blue, right). Bottom right: voltage response of the cell to hyper- to depolarizing current pulses. Scale bars, 5 µm (left inset); 10 µm (right insets).

(B) Trains of bAPs (top) evoked by brief pulses (1 nA, 1 ms, 200 Hz) in the SOM-IN resulted in Ca^{2+}-transients (bottom) under control conditions (left, gray), in baclofen (10 µM, middle, in black) and CGP (5 µM, right, in black).

(C) Summary of peak Ca^{2+}-transients during control (Ctrl), baclofen (Bac), and CGP in 5 SOM-INs from juvenile rats (P17–P25).

(D) Ca^{2+}-transient amplitudes during control condition, application of nifedipine (Nif) and co-application of nifedipine and baclofen (Bac+Nif) from 5 SOM-INs.

(E) Bar chart of normalized Ca^{2+}-transients during application of Bac, Nif, Nif+Bac, and CGP in juvenile rats.

(F) Ca^{2+}-transients (bottom) evoked by bAP trains (top) in a SOM-IN from an adult rat under control conditions (left, gray) in baclofen (middle, in black) and CGP (right, in black).

(G) Summary of peak Ca^{2+}-transients during control (Ctrl), in baclofen (Bac) and CGP in 9 SOM-INs from adult rats (P50–P60).

(H) Bar chart of normalized Ca^{2+}-transient amplitudes in Bac and CGP in juvenile rats.

Bar charts show mean ± SEM. Data from individual cells is superimposed on bars (open circles); numbers of tested cells are in parentheses. ns, $p > 0.05$; *$p < 0.05$; **$p < 0.01$.

See also Figures S3 and S4.

(10 cells) resulted in a 27.8% ± 6.5% reduction in the Ca^{2+} response ($t_{(9)} = 4.25$; $p = 0.002$, Wilcoxon test), which recovered in CGP (5 µM; $t_{(4)} = 0.08$; $p = 0.94$, Wilcoxon test) (Figures 2B and 2C).

To confirm that L-type VGCCs contribute to Ca^{2+}-transients, we applied the selective blocker nifedipine (10 µM), resulting in a 13.2% ± 4.2% reduction in the signal ($t_{(4)} = 3.20$; $p = 0.033$, Wilcoxon test) (Figure 2D), comparable to baclofen effect ($t_{(10,5)} = 1.35$; $p = 0.57$, one-way ANOVA). Moreover, co-application of baclofen and nifedipine did not further reduce the Ca^{2+} signal ($t_{(10,9)} = 1.02$; $p = 0.68$) (Figures 2D and 2E), independent of whether the co-application followed an initial baclofen ($t_{(4,4)} = 1.05$; $p = 0.62$, Holm-Sidak's post-test) or nifedipine application ($t_{(6,6)} = 1.39$; $p = 0.22$, Holm-Sidak's post-test). This mutual occlusion indicates that $GABA_BRs$ predominantly inhibit L-type VGCCs in SOM-IN dendrites. This result was verified using 1-photon imaging, using the same pharmacological treatment (Figure S4). Furthermore, $GABA_BR$ inhibition of Ca^{2+}-transients was maintained into adulthood (Figures 2F–2H).

$GABA_BRs$ and $Ca_V1.2$ Channels Preferentially Cluster on Dendritic Shafts of mGluR1α-Expressing Cells

Our data indicate that $GABA_BRs$ modulate L-type VGCCs but not Kir3 channels in SOM-INs. Therefore, we next examined the distribution, density, and spatial relationship of $GABA_BR$, Kir3, and $Ca_V1.2$ channel on SOM-IN dendrites by quantitative SDS-FRL electron microscopy, using mGluR1α as a surface marker for SOM-INs (Baude et al., 1993). Immunoreactivity for the $GABA_{B1}$ subunit was consistently observed at mGluR1α-positive dendrites (Figure 3A), with a density of 49.1 ± 4.5 particles/µm^2

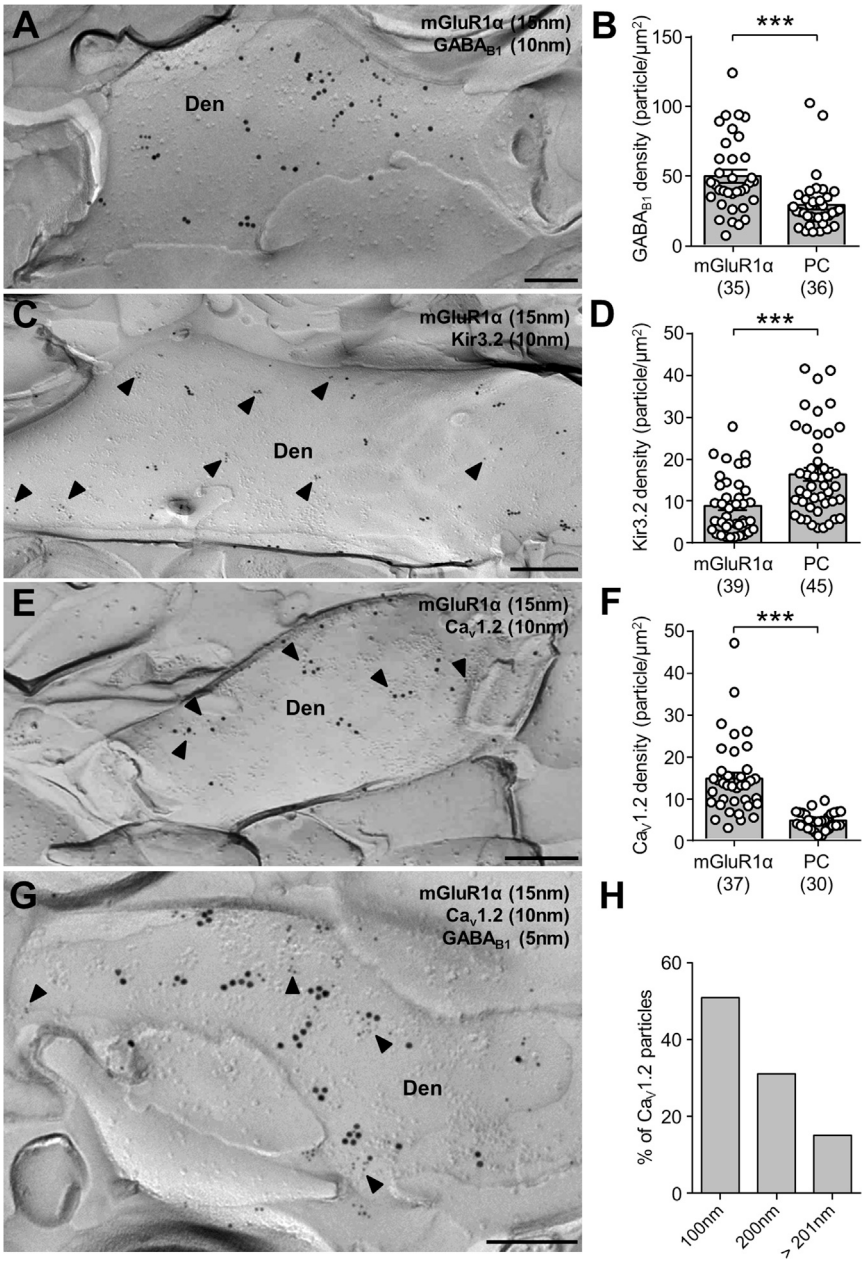

Figure 3. Differential Surface Densities of GABA$_{B1}$, Kir3.2, and Ca$_V$1.2 on Putative SOM-IN Dendrites

(A, C, and E) SDS-FRL electron micrographs illustrating the distribution of GABA$_{B1}$ (A), Kir3.2 (C), and Ca$_V$1.2 (E) (all 10 nm gold particles, arrowheads in C and E) on mGluR1α-expressing (15 nm) dendrites (Den).

(B, D, and F) Summary bar charts of the surface densities of GABA$_{B1}$ (B), Kir3.2 (D), and Ca$_V$1.2 (F) particles on mGluR1α-positive dendrites, compared to CA1 PCs. Numbers of dendrites are in parentheses.

(G) Immunogold labeling for GABA$_{B1}$ (5 nm particles, arrowheads) and Ca$_V$1.2 (10 nm) on a mGluR1α-immunoreactive (15 nm) dendrite.

(H) Distribution of Ca$_V$1.2 relative to GABA$_{B1}$ particles, plotted as percentage against their distance to nearest GABA$_{B1}$ particles in 100-nm bins.

Bar charts show mean ± SEM. Data from individual cells is shown (open circles); numbers of tested cells are in parentheses. ***$p < 0.001$. Scale bars, 200 nm (A, E, and G) and 100 nm (C).

(35 dendrites from 3 animals), higher than that of CA1 PCs in the same replicas (28.5 ± 3.2 particles/μm^2, 36 dendrites, $U_{(34,35)}$ = 287.0; $p < 0.0001$, Mann-Whitney test) (Figure 3B). In contrast, Kir3 channel subunit density was 8.6 ± 1.1 particles/μm^2 on mGluR1α dendrites (39 dendrites from 3 animals) (Figure 3C), ~50% lower than on neighboring PCs (16.2 ± 1.6 particles/μm^2, 45 dendrites, $U_{(38,44)}$ = 459.0; $p = 0.0001$, Mann-Whitney test) (Figure 3D), explaining the small GABA$_B$R-mediated currents in SOM-INs.

Next, we determined the surface expression of Ca$_V$1.2, which was observed on mGluR1α-positive dendrites (Figure 3E) with a density of 14.3 ± 1.5 particles/μm^2 (37 dendrites from 3 animals) (Figure 3F), over 3-fold higher than on PCs (4.3 ± 0.4 particles/μm^2, 30 dendrites, $U_{(36,29)}$ = 77.0; $p < 0.0001$). Finally, to examine the spatial relationship between GABA$_{B1}$ and Ca$_V$1.2 we performed triple labeling for mGluR1α, GABA$_{B1}$ and Ca$_V$1.2 (Figure 3G) and measured the proximity of Ca$_V$1.2 particles to the closest GABA$_{B1}$ particle. This analysis revealed that 51% of Ca$_V$1.2 subunit-containing channels were located within 100 nm of a GABA$_{B1}$ subunit (Figure 3H). Thus, GABA$_{B1}$ and Ca$_V$1.2 subunits are present at high density and colocalize on SOM-IN dendrites.

Postsynaptic GABA$_B$R Activation Inhibits Synaptic Plasticity in SOM-INs

Long-term potentiation (LTP) at excitatory synapses onto SOM-INs critically depends on L-type VGCC activation (Topolnik et al., 2009). Therefore, we asked if associative LTP in SOM-INs is sensitive to GABA$_B$R activation. EPSC amplitudes were potentiated to 163.8% ± 17.3% (measured at 20–25 min; $t_{(6)}$ = 3.99; $p = 0.007$, t test, 7 cells) (Figure 4A) following LTP induction in SOM-INs. When baclofen was pre-applied, the same stimulus did not potentiate EPSCs (mean EPSC amplitude: 95.8% ± 10.8% of baseline; $t_{(5)} = 0.47$; $p = 0.66$, t test, Wilcoxon test, 6 cells) (Figures 4B and 4F). A comparable GABA$_B$R-mediated inhibition of LTP was observed in adult rats (Figures 4C, 4D, and 4F).

To confirm that the LTP observed was dependent on L-type VGCCs, as previously shown (Topolnik et al., 2009), we pre-applied nifedipine (10 μM) to 6 SOM-INs. As expected, this manipulation fully abolished LTP (EPSC: 89.2 ± 11.0% of baseline $t_{(5)}$ = 1.07; $p = 0.33$, t test) (Figures 4E and 4F). These data,

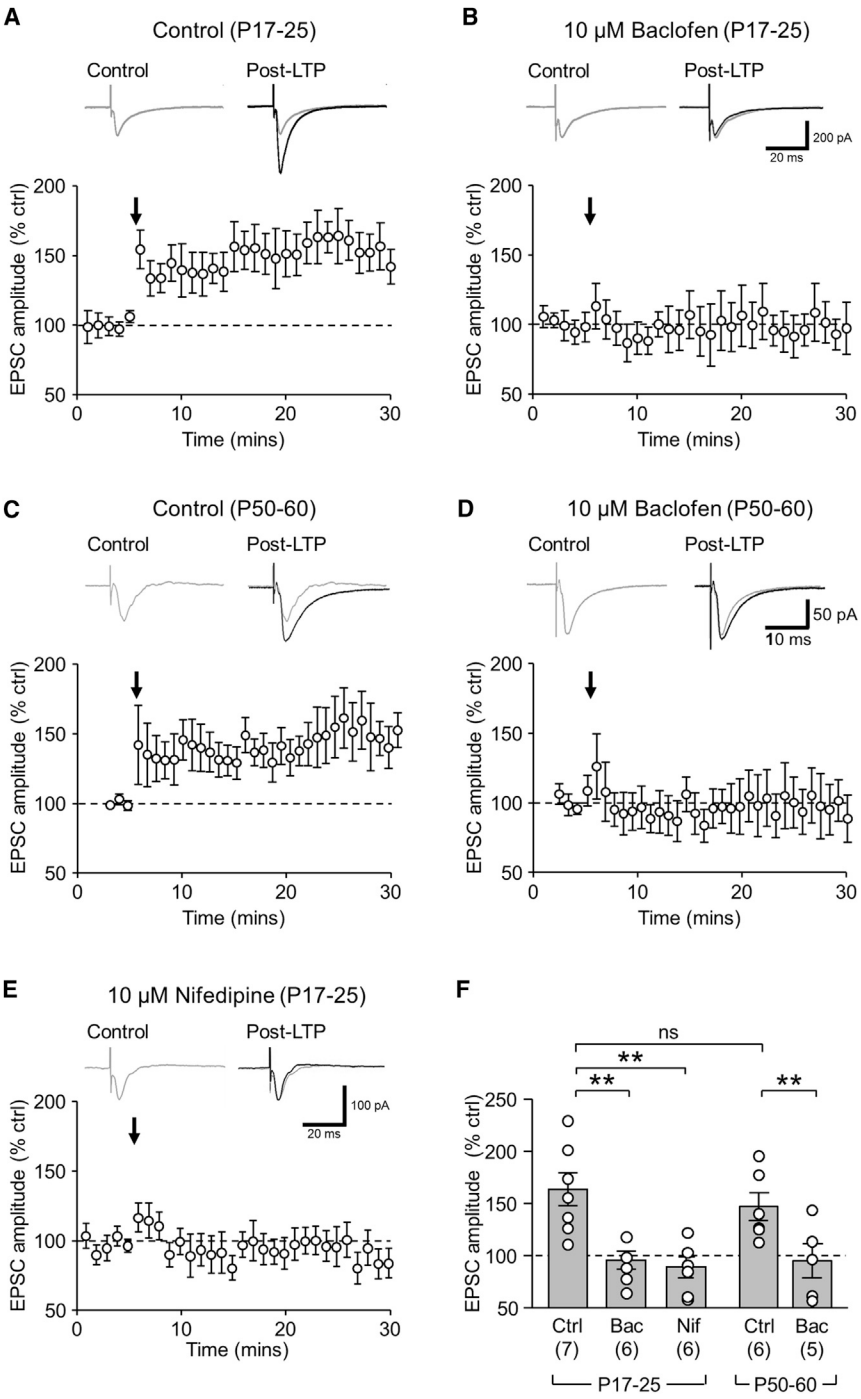

Figure 4. Postsynaptic $GABA_BR$ Activation Abolishes LTP in SOM-INs

(A and C) Time course plots of normalized EPSC amplitude in SOM-INs before and after LTP induction (TBS, arrow at 5 min) in slices from juvenile (P17–P25) (A, 7 cells) and adult rats (P50–P60) (C, 6 cells). Example traces corresponding to control (in gray) and LTP (25–30 min, in black) are shown above.

(B and D) Time course of the normalized EPSC amplitudes following LTP induction in SOM-INs in the presence of baclofen (10 μM) in juvenile (B, 6 cells) and adult animals (D, 5 cells).

(E) Time course of EPSC amplitudes following LTP induction in the presence of nifedipine (10 μM) in juvenile animals (6 cells).

(F) Summary of normalized EPSC amplitudes following LTP induction under control (Ctrl) and in the presence of baclofen (Bac, 10 μM) or nifedipine (Nif, 10 μM) in SOM-INs from juvenile and adult rats. Dashed line indicates baseline; cell numbers are in parentheses.

Bar charts show mean ± SEM. **p < 0.01.

thus, demonstrate that activation of postsynaptic $GABA_BRs$, via inhibition of $Ca_V1.2$ Ca^{2+} channels, abolishes postsynaptic LTP induction at excitatory synapses onto SOM-INs.

DISCUSSION

In the present study, we provide compelling evidence that $GABA_BRs$ are present on dendritic membranes of CA1 SOM-INs, but do not activate the canonical Kir3 signaling cascade. Rather, $GABA_BRs$ cluster with and inhibit L-type VGCCs, reducing dendritic calcium influx and blocking LTP at excitatory synapses onto SOM-INs. This effect will preclude synaptic strengthening during network activation, a mechanism by which $GABA_BRs$ can contribute to a long-term alteration of excitation and inhibition balance in the network.

Small $GABA_BR$-Mediated Inhibitory Currents in SOM-INs

The major $GABA_BR$ signaling in postsynaptic compartments has long been considered to involve Kir3 channels (Lüscher et al., 1997; Kaupmann et al., 1998; Degro et al., 2015). In contrast, while we find that $GABA_BRs$ and Kir3 channels are present on SOM-IN dendrites, only very small K^+ currents were produced, partially explained by a lower Kir3 channel expression. In a network context, the small $GABA_BR$ currents in SOM-INs are consistent with observations in other dendritic-targeting IN types: parvalbumin bistratified cells (Booker et al., 2013) and cholecystokinin INs (Booker et al., 2017) and may be a common principle for dendritic-targeting INs. This divergence between perisomatic and dendritic inhibitory INs implies that $GABA_BR$ activation shifts inhibition between the two target compartments.

Colocalization and Negative Coupling of $GABA_BRs$ and VGCCs in SOM-INs

We provide evidence that postsynaptic $GABA_BRs$ preferentially signal through and inhibit VGCCs in SOM-INs. The high

expression of $Ca_V1.2$ and nifedipine-sensitive Ca^{2+}-transients further indicate that these channels substantially contribute to Ca^{2+} influx in SOM-IN dendrites. In fact, $GABA_BRs$ have been shown to inhibit VGCCs, as an alternative postsynaptic effector in PC dendrites (Sabatini and Svoboda, 2000; Chalifoux and Carter, 2011; Pérez-Garci et al., 2013). The co-clustering of the $GABA_{B1}$ subunits with the $Ca_V1.2$ (L-type) VGCCs subunit is a structural correlate of this interaction in SOM-IN dendrites and may reflect a tight functional coupling through a membrane delimited $G_{i/o}$-$\beta\gamma$ interaction (Pérez-Garci et al., 2013). Whether these mechanisms also apply to dendritic spines remains an open question.

$GABA_BR$ Signaling Abolishes Synaptic Plasticity in SOM-INs

By negatively coupling to L-type VGCCs, $GABA_BRs$ block the induction of LTP in SOM-INs, adding to the wide repertoire of molecular mechanisms involved in synaptic plasticity in these INs (Topolnik et al., 2006; Nicholson and Kullmann, 2014; Vasuta et al., 2015). The form of plasticity is dependent on the activity pattern (Lamsa et al., 2007) that is plausibly translated into a differential activation of glutamate receptors and downstream signaling cascades (Topolnik et al., 2005, 2006, 2009; Oren et al., 2009). Indeed, L-type VGCCs potentiation by group I mGluRs promotes LTP in SOM-INs (Topolnik et al., 2009). In cerebellar Purkinje cells, $GABA_BRs$ facilitate mGluR1 activation (Hirono et al., 2001). In SOM-INs, the two receptors converge on L-type VGCCs, but exert opposing actions: $GABA_BRs$ intercept mGluR-mediated signaling by inhibiting L-type channels and thereby abolish LTP induction.

Inhibition of LTP in SOM-INs by $GABA_BRs$ is in stark contrast to the facilitation of LTP by $GABA_BR$ activation observed in PCs (Davies et al., 1991; Mott and Lewis, 1991). In fact, despite their inhibitory nature, $GABA_BRs$ can produce disinhibitory effects in cortical networks due to a preferential inhibition of INs and their output synapses (Foster et al., 2013; Papatheodoropoulos, 2015). In SOM-INs, $GABA_BRs$ do not produce hyperpolarization, but prevent the induction of LTP and thereby preclude an enhanced recruitment of the feedback circuit. Considering that the main output of SOM-INs is onto PC distal dendrites, this reduced recruitment will allow increased synaptic transmission onto CA1 PCs and may lead to a breakdown of the specificity of spatial information carried by entorhinal inputs onto CA1 PCs (Leão et al., 2012) via activation of $GABA_BRs$ on nearby pre- and postsynaptic elements, as previously described in the neocortex (Urban-Ciecko et al., 2015). Indeed, prior studies have shown that $GABA_BR$ activation is capable of impairing hippocampal-dependent spatial learning (McNamara and Skelton, 1996; Arolfo et al., 1998), consistent with the importance of this circuit.

EXPERIMENTAL PROCEDURES

Electrophysiological Recordings

A full description of methods can be found in the Supplemental Information. In brief, 300-μm acute hippocampal slices were prepared from juvenile (17- to 25-day-old) and adult (50- to 60-day-old) male Wistar rats (Booker et al., 2014, 2017). All experiments were performed in accordance with institutional, local governmental (LaGeSo, Berlin T 0215/11; LaGeSo, Freiburg X-14/11H) and national guidelines (German Animal Welfare Act; ASPA, United Kingdom Home Office). Whole-cell recordings were made using pipettes filled with K-gluconate-based solution at 32°C ± 1°C. $GABA_BR$-mediated currents were measured in the presence of the ionotropic receptor blockers NBQX, CNQX or DNQX, DL-APV, and bicuculline, gabazine, or picrotoxin at a holding potential of −65 mV. Synaptic currents were elicited by a glass monopolar electrode in *str. oriens*.

For Ca^{2+}-imaging, we used 2-photon microcopy with pipettes filled with intracellular solution containing BAPTA-OGB1 and a morphometric dye. Ca^{2+} transients were measured in proximal dendrites following trains of 4 APs to evoke Ca^{2+} influx, line-scans were recorded at ~200 Hz. Baclofen or nifedipine was applied to the bath; CGP was applied following baclofen to confirm receptor specificity.

LTP was induced at inputs to SOM-INs with EPSCs elicited by a monopolar electrode placed in the alveus. Theta-burst stimulation was paired with a postsynaptic depolarization to −20 mV, repeated 3 times at 30-s intervals. In a subset of experiments, baclofen or nifedipine were pre-applied to the bath, and the EPSC was titrated to match control recordings. All neurons were filled with biocytin during recordings, fixed overnight, labeled with streptavidin and antibodies to SOM, and imaged with confocal microcopy.

Electron Microscopy

Electron microscopic analysis was performed on 60-day-old wild-type Wistar rats (Althof et al., 2015). Coronal hippocampal sections were cut, cryoprotected, and blocks of *str. oriens/alveus* of CA1 were dissected and frozen under high-pressure. Samples were fractured and coated with carbon and platinum in a freeze-fracture replica machine. Replicas were then digested, washed, blocked, and then incubated with subunit-specific primary antibodies followed by incubation with gold-coupled secondary antibodies. Strongly mGluR1α-immunoreactive and CA1 PC dendrites in *str. oriens* were imaged and analyzed.

Statistics

All data are shown as mean ± SEM. Analysis was performed in GraphPad Prism 3.0 (GraphPad Software, CAUSA). For all electrophysiology data, "n" refers to the number of recorded cells; for electron microscopy "n" refers to the number of dendrites tested from 3–4 rats. Group data were compared with one-way ANOVA test combined with Holm's-Sidak post-test. Analysis of unpaired and paired data was performed with Mann-Whitney or Wilcoxon matched-pairs tests, respectively. Significance was assumed if $p < 0.05$.

SUPPLEMENTAL INFORMATION

Supplemental Information includes Supplemental Experimental Procedures and four figures and can be found with this article online at https://doi.org/10.1016/j.celrep.2017.12.021.

ACKNOWLEDGMENTS

We thank Natalie Wernet, Julia Bank, and Ina Wolter for excellent technical support. Funding was provided by DFG (FOR 2134 to I.V. and A.K.), BIOSS-2 (to A.K.), McNaught Bequest (to I.V. and S.A.B.), Tenovus Scotland (to I.V.), MRC (to S.A.B., D.J.A.W., and P.C.K.), The Patrick Wild Centre for Autism Research (to S.A.B., D.J.A.W., and P.C.K.), and the Dame Stephanie Shirley Foundation (to S.A.B., D.J.A.W., and P.C.K.).

AUTHOR CONTRIBUTIONS

S.A.B., D.L., D.J.A.W., P.C.K., A.K., and I.V. designed experiments. S.A.B. and A.L.G. performed electrophysiological experiments and analyzed data. A.K. and D.L. performed SDS-FRL and analyzed data. M.W. provided antibodies. S.A.B., D.L., D.J.A.W., P.C.K., A.K., and I.V. wrote the manuscript.

DECLARATION OF INTERESTS

The authors declare no competing interests.

Received: July 12, 2017
Revised: October 14, 2017
Accepted: December 6, 2017
Published: January 2, 2018

REFERENCES

Althof, D., Baehrens, D., Watanabe, M., Suzuki, N., Fakler, B., and Kulik, Á. (2015). Inhibitory and excitatory axon terminals share a common nanoarchitecture of their $Ca_v2.1$ (P/Q-type) $Ca^{(2+)}$ channels. Front. Cell. Neurosci. *9*, 315.

Arolfo, M.P., Zanudio, M.A., and Ramirez, O.A. (1998). Baclofen infused in rat hippocampal formation impairs spatial learning. Hippocampus *8*, 109–113.

Baude, A., Nusser, Z., Roberts, J.D.B., Mulvihill, E., McIlhinney, R.A., and Somogyi, P. (1993). The metabotropic glutamate receptor (mGluR1 α) is concentrated at perisynaptic membrane of neuronal subpopulations as detected by immunogold reaction. Neuron *11*, 771–787.

Booker, S.A., Gross, A., Althof, D., Shigemoto, R., Bettler, B., Frotscher, M., Hearing, M., Wickman, K., Watanabe, M., Kulik, Á., and Vida, I. (2013). Differential GABAB-receptor-mediated effects in perisomatic- and dendrite-targeting parvalbumin interneurons. J. Neurosci. *33*, 7961–7974.

Booker, S.A., Song, J., and Vida, I. (2014). Whole-cell patch-clamp recordings from morphologically- and neurochemically-identified hippocampal interneurons. J. Vis. Exp. *2014*, e51706.

Booker, S.A., Althof, D., Gross, A., Loreth, D., Müller, J., Unger, A., Fakler, B., Varro, A., Watanabe, M., Gassmann, M., et al. (2017). KCTD12 auxiliary proteins modulate kinetics of GABAB receptor-mediated inhibition in cholecystokinin-containing interneurons. Cereb. Cortex *27*, 2318–2334.

Chalifoux, J.R., and Carter, A.G. (2011). GABAB receptor modulation of voltage-sensitive calcium channels in spines and dendrites. J. Neurosci. *31*, 4221–4232.

Davies, C.H., Starkey, S.J., Pozza, M.F., and Collingridge, G.L. (1991). GABA autoreceptors regulate the induction of LTP. Nature *349*, 609–611.

de Lanerolle, N.C., Kim, J.H., Robbins, R.J., and Spencer, D.D. (1989). Hippocampal interneuron loss and plasticity in human temporal lobe epilepsy. Brain Res. *495*, 387–395.

Degro, C.E., Kulik, A., Booker, S.A., and Vida, I. (2015). Compartmental distribution of GABAB receptor-mediated currents along the somatodendritic axis of hippocampal principal cells. Front. Synaptic Neurosci. *7*, 6.

Dugladze, T., Vida, I., Tort, A.B., Gross, A., Otahal, J., Heinemann, U., Kopell, N.J., and Gloveli, T. (2007). Impaired hippocampal rhythmogenesis in a mouse model of mesial temporal lobe epilepsy. Proc. Natl. Acad. Sci. USA *104*, 17530–17535.

Foster, J.D., Kitchen, I., Bettler, B., and Chen, Y. (2013). GABAB receptor subtypes differentially modulate synaptic inhibition in the dentate gyrus to enhance granule cell output. Br. J. Pharmacol. *168*, 1808–1819.

Gloveli, T., Dugladze, T., Saha, S., Monyer, H., Heinemann, U., Traub, R.D., Whittington, M.A., and Buhl, E.H. (2005). Differential involvement of oriens/pyramidale interneurones in hippocampal network oscillations in vitro. J. Physiol. *562*, 131–147.

Hirono, M., Yoshioka, T., and Konishi, S. (2001). GABA(B) receptor activation enhances mGluR-mediated responses at cerebellar excitatory synapses. Nat. Neurosci. *4*, 1207–1216.

Katona, I., Acsády, L., and Freund, T.F. (1999). Postsynaptic targets of somatostatin-immunoreactive interneurons in the rat hippocampus. Neuroscience *88*, 37–55.

Kaupmann, K., Malitschek, B., Schuler, V., Heid, J., Froestl, W., Beck, P., Mosbacher, J., Bischoff, S., Kulik, A., Shigemoto, R., et al. (1998). GABA(B)-receptor subtypes assemble into functional heteromeric complexes. Nature *396*, 683–687.

Klausberger, T., and Somogyi, P. (2008). Neuronal diversity and temporal dynamics: the unity of hippocampal circuit operations. Science *321*, 53–57.

Lamsa, K.P., Heeroma, J.H., Somogyi, P., Rusakov, D.A., and Kullmann, D.M. (2007). Anti-Hebbian long-term potentiation in the hippocampal feedback inhibitory circuit. Science *315*, 1262–1266.

Leão, R.N., Mikulovic, S., Leão, K.E., Munguba, H., Gezelius, H., Enjin, A., Patra, K., Eriksson, A., Loew, L.M., Tort, A.B.L., and Kullander, K. (2012). OLM interneurons differentially modulate CA3 and entorhinal inputs to hippocampal CA1 neurons. Nat. Neurosci. *15*, 1524–1530.

Lüscher, C., Jan, L.Y., Stoffel, M., Malenka, R.C., and Nicoll, R.A. (1997). G protein-coupled inwardly rectifying K+ channels (GIRKs) mediate postsynaptic but not presynaptic transmitter actions in hippocampal neurons. Neuron *19*, 687–695.

McBain, C.J., DiChiara, T.J., and Kauer, J.A. (1994). Activation of metabotropic glutamate receptors differentially affects two classes of hippocampal interneurons and potentiates excitatory synaptic transmission. J. Neurosci. *14*, 4433–4445.

McNamara, R.K., and Skelton, R.W. (1996). Baclofen, a selective GABAB receptor agonist, dose-dependently impairs spatial learning in rats. Pharmacol. Biochem. Behav. *53*, 303–308.

Mott, D.D., and Lewis, D.V. (1991). Facilitation of the induction of long-term potentiation by GABAB receptors. Science *252*, 1718–1720.

Müller, C., and Remy, S. (2014). Dendritic inhibition mediated by O-LM and bistratified interneurons in the hippocampus. Front. Synaptic. Neurosci. *6*, 23.

Nicholson, E., and Kullmann, D.M. (2014). Long-term potentiation in hippocampal oriens interneurons: postsynaptic induction, presynaptic expression and evaluation of candidate retrograde factors. Philos Trans. R. Soc. Lond. B. Biol. Sci. *369*, 20130133.

Oren, I., Nissen, W., Kullmann, D.M., Somogyi, P., and Lamsa, K.P. (2009). Role of ionotropic glutamate receptors in long-term potentiation in rat hippocampal CA1 oriens-lacunosum moleculare interneurons. J. Neurosci. *29*, 939–950.

Papatheodoropoulos, C. (2015). Higher intrinsic network excitability in ventral compared with the dorsal hippocampus is controlled less effectively by GABAB receptors. BMC Neurosci. *16*, 75.

Pérez-Garci, E., Larkum, M.E., and Nevian, T. (2013). Inhibition of dendritic Ca2+ spikes by GABAB receptors in cortical pyramidal neurons is mediated by a direct Gi/o-β-subunit interaction with Cav1 channels. J. Physiol. *591*, 1599–1612.

Sabatini, B.L., and Svoboda, K. (2000). Analysis of calcium channels in single spines using optical fluctuation analysis. Nature *408*, 589–593.

Sloviter, R.S., Ali-Akbarian, L., Elliott, R.C., Bowery, B.J., and Bowery, N.G. (1999). Localization of GABA(B) (R1) receptors in the rat hippocampus by immunocytochemistry and high resolution autoradiography, with specific reference to its localization in identified hippocampal interneuron subpopulations. Neuropharmacology *38*, 1707–1721.

Standaert, D.G., Landwehrmeyer, G.B., Kerner, J.A., Penney, J.B., Jr., and Young, A.B. (1996). Expression of NMDAR2D glutamate receptor subunit mRNA in neurochemically identified interneurons in the rat neostriatum, neocortex and hippocampus. Brain Res. Mol. Brain Res. *42*, 89–102.

Topolnik, L., Congar, P., and Lacaille, J.-C. (2005). Differential regulation of metabotropic glutamate receptor- and AMPA receptor-mediated dendritic Ca2+ signals by presynaptic and postsynaptic activity in hippocampal interneurons. J. Neurosci. *25*, 990–1001.

Topolnik, L., Azzi, M., Morin, F., Kougioumoutzakis, A., and Lacaille, J.-C. (2006). mGluR1/5 subtype-specific calcium signalling and induction of long-term potentiation in rat hippocampal oriens/alveus interneurones. J. Physiol. *575*, 115–131.

Topolnik, L., Chamberland, S., Pelletier, J.-G., Ran, I., and Lacaille, J.-C. (2009). Activity-dependent compartmentalized regulation of dendritic Ca2+ signaling in hippocampal interneurons. J. Neurosci. *29*, 4658–4663.

Tyan, L., Chamberland, S., Magnin, E., Camiré, O., Francavilla, R., David, L.S., Deisseroth, K., and Topolnik, L. (2014). Dendritic inhibition provided by interneuron-specific cells controls the firing rate and timing of the hippocampal feedback inhibitory circuitry. J. Neurosci. *34*, 4534–4547.

Urban-Ciecko, J., Fanselow, E.E., and Barth, A.L. (2015). Neocortical somatostatin neurons reversibly silence excitatory transmission via GABAb receptors. Curr. Biol. *25*, 722–731.

Vasuta, C., Artinian, J., Laplante, I., Hébert-Seropian, S., Elayoubi, K., and Lacaille, J.-C. (2015). Metaplastic regulation of CA1 Schaffer collateral pathway plasticity by Hebbian mGluR1a-mediated plasticity at excitatory synapses onto somatostatin-expressing interneurons. eNeuro *2*, ENEURO.0051-15.2015.

Wang, A.Y., Lohmann, K.M., Yang, C.K., Zimmerman, E.I., Pantazopoulos, H., Herring, N., Berretta, S., Heckers, S., and Konradi, C. (2011). Bipolar disorder type 1 and schizophrenia are accompanied by decreased density of parvalbumin- and somatostatin-positive interneurons in the parahippocampal region. Acta Neuropathol. *122*, 615–626.